Reactivity of Phosphate Diesters Doubly Coordinated to a Dinuclear Cobalt(III) Complex: Dependence of the Reactivity on the Basicity of the Leaving Group

Nicholas H. Williams,*,† William Cheung,‡ and Jik Chin*,‡

Contribution from the Department of Chemistry, Sheffield University, Sheffield S3 7HF, U.K., and Department of Chemistry, McGill University, Montreal, Canada H3A 2K6

Received February 27, 1998

Abstract: Reactivities of eight phosphate diesters each coordinated to a dinuclear Co(III) complex were investigated ($[Co_2(tacn)_2(OH)_2\{O_2P(OR)_2\}]^{3+}$; tacn = 1,4,7-triazacyclononane). Four of the complexes were coordinated by substituted phenyl methyl phosphates (substituent *m*-F, *p*-NO_2 (**1a**); *p*-NO_2 (**1b**); *m*-NO_2 (**1c**); unsubstituted (**1d**)) and two by substituted phenyl 2-hydroxypropyl phosphates (substituent *p*-NO_2 (**2a**); unsubstituted (**2b**)). Reactivities of dialkyl phosphates coordinated to the dinuclear Co(III) complex (1,2-propylene phosphate (**3**); dimethyl phosphate (**4**)) were also investigated. Hydrolysis of the phosphate diesters in **1a** to **1d** takes place by intramolecular oxide attack on the bridging phosphate while hydrolysis of **3** principally takes place by intermolecular hydroxide attack on the bridging phosphate. The diester in **2a** cleaves by intramolecular oxide attack while that in **2b** cleaves by intramolecular transesterification. Dimethyl phosphate dissociates from **4** without any observable cleavage of the diester. These results can be understood in terms of the More O'Ferrall−Jencks energy diagram, and they indicate that there will be considerable cooperativity between the oxide activation and leaving group activation.

Introduction

In nature there are many enzymes that hydrolyze phosphate esters that are activated by two or more metal ions. They include ribozymes and phosphate mono-, di-, and triesterases that cleave phosphate esters with good or poor leaving groups.[1] Model studies have shown that simple dinuclear metal complexes can provide enormous rate accelerations for hydrolyzing phosphate esters, shedding light on how metal ions may promote these reactions.[2] In preliminary communications, we reported that *p*-nitrophenyl methyl phosphate coordinated to the dinuclear Co(III) complex (**1b**) is hydrolyzed about 10^{11} times more rapidly than the corresponding uncoordinated phosphate diester.[3] ^{18}O labeling experiments revealed that the mechanism of the hydrolysis reaction involves nucleophilic attack of the bridging phosphate diester by the bridging oxide. Hence, the enormous rate acceleration is due to the intramolecular oxide in combination with double Lewis acid activation of the diester. In contrast to the exceptional rate acceleration above, the phosphate diester in **2b** is cleaved by intramolecular transesterification only about 10^5 times more rapidly than the corresponding uncoordinated phosphate diester,[4] and so double Lewis acid activation by itself provides about 10^5-fold rate acceleration for the cleavage of this diester. Although Co(III) does not appear to be used by metalloenzymes for phosphate hydrolysis (but has been reported as a cofactor for nitrile hydratases[5]), a wide variety of metal ions can be used to activate this type of enzyme (Mg(II), Ca(II), Zn(II), Co(II), Fe(II), Fe(III), Mn(II), and Cd(II) are all naturally used or are good substitutions). Hence, it is unlikely that the unique properties of one ion are required to catalyze phosphate hydrolysis efficiently. We have used Co(III) here as it provides the opportunity for detailed mechanistic analysis; the isolated complexes have clearly defined substrate−metal ion interactions, and the relative substitutional inertness of these complexes allows unambiguous analysis.

It is of considerable interest to understand hydrolysis of phosphate esters not only with good leaving groups, but also with poor leaving groups, since both kinds of phosphate esters are found in biologically important molecules. Furthermore, it is also valuable to probe the structures of the transition states involved in these reactions, as they are likely to contrast with the background reaction in the absence of promotion by metal ions. Such studies may extend our understanding of these reactions and aid in the future development of models and artificial catalysts. In this paper we investigate the dependence of the rate acceleration for phosphate diester cleavage on the

† Sheffield University.
‡ McGill University.

(1) (a) Sträter, N.; Lipscomb, W. N.; Klabunde, T.; Krebs, B. *Angew. Chem., Int. Ed. Engl.* **1996**, *35*, 2024. (b) Wilcox, D. E. *Chem. Rev.* **1996**, *96*, 2435.

(2) (a) Göbel, M. W. *Angew. Chem., Int. Ed. Engl.* **1994**, *33*, 1141. (b) Chapman, W. H.; Breslow, R. *J. Am. Chem. Soc.* **1995**, *117*, 5462. (c) Wall, M.; Hynes, R. C.; Chin, J. *Angew. Chem., Int. Ed. Engl.* **1993**, *32*, 1633. (d) Young, M. J.; Chin, J. *J. Am. Chem. Soc.* **1995**, *117*, 10577. (e) Molenveld, P.; Kapsabelis, S.; Engbersen, J. F. J.; Reinhoudt, D. N. *J. Am. Chem. Soc.* **1997**, *119*, 2948. (f) Ragunathan, K. G.; Schneider, H.-J. *Angew. Chem., Int. Ed. Engl.* **1996**, *35*, 1219. (g) Yashiro, M.; Ishikubo, A.; Komiyama, M. *J. Chem. Soc., Chem. Commun.* **1995**, 1793. (h) Liu, S.; Luo, Z.; Hamilton, A. D. *Angew. Chem., Int. Ed. Engl.* **1997**, *36*, 2678. (i) Koike, T.; Inoue, M.; Kimura, E.; Shiro, M. *J. Am. Chem. Soc.* **1996**, *118*, 3091.

(3) Wahnon, D.; Lebuis, A.-M.; Chin, J. *Angew. Chem., Int. Ed. Engl.* **1995**, *34*, 2412.

(4) Williams, N.; Chin, J. *J. Chem. Soc., Chem. Commun.* **1996**, 131.

(5) (a) Brennan, B. A.; Alms, G.; Nelson, M. J.; Durney, L. T.; Scarrow, R. C. *J. Am. Chem. Soc.* **1996**, *118*, 9194. (b) Payne, M. S.; Wu, S.; Fallon, R. D.; Tudor, G.; Stieglitz, B.; Turner, Jr., I. M.; Nelson, M. J. *Biochemistry* **1997**, *36*, 5447.

S0002-7863(98)00660-X CCC: $15.00
Published on Web 07/31/1998

basicity of the leaving group by studying the reactivities of **1a** to **1d**, **2a**, **2b**, **3**, and **4**. Our aim is to dissect quantitatively how much rate acceleration is due to the oxide nucleophile and how much is due to double Lewis acid activation for the cleavage of phosphate diesters.

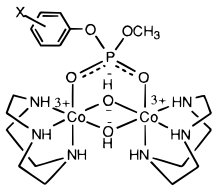

1a: X = m-F, p-NO_2
1b: X = p-NO_2
1c X = m-NO_2
1d: X = H

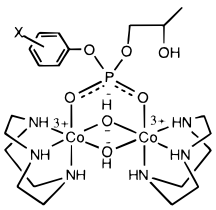

2a: X = p-NO_2
2b: X = H

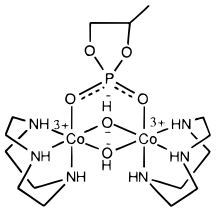

3

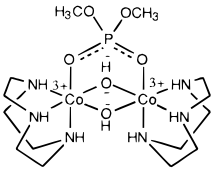

4

Experimental Section

Instruments. ^{1}H NMR (200 MHz) and ^{13}C NMR (50.3 MHz) spectra were obtained with a Gemini 200 spectrometer, while ^{31}P NMR spectra were obtained with a Varian XL-300 FT spectrometer (121.4 MHz) or a Varian Unity 500 FT spectrometer (202.5 MHz). Chemical shifts are reported in ppm with 3-(trimethylsilyl)-1-propanesulfonic acid (0 ppm), trimethyl phosphate (0 ppm), and dioxane (67.4 ppm) used as references for ^{1}H, ^{31}P, and ^{13}C NMR, respectively.

Kinetic studies were carried out by a UV−vis method with a Hewlett-Packard 8452A diode array spectrophotometer equipped with a Lauda RM6 thermostat. Product analyses by HPLC were performed on a Hewlett-Packard 1090 series II liquid chromatograph using a 2.1 mm × 100 mm Hypersil ODS C-18 reversed-phase column.

Materials. The sodium, barium, or *tert*-butylammonium salts of the phosphate diesters in **1** and **2** were prepared according to literature procedures.[6] Dinuclear Co(III) complexes **1**, **2**, and **4** were prepared by the same method as previously reported for the synthesis of **1a**, **2b**, and **4**.[3,4] Complex **3** was generated in situ from **2b** and used without isolation. In all cases, the complexed diester showed the characteristic ∼14 ppm downfield shift relative to the unbound diester in the ^{31}P NMR.

General Procedure for Synthesis of 1, 2, and 4. [(1,4,7-Triazacyclononane)$_2$Co$_2$(OH)$_3$](ClO$_4$)$_3$[7] (25 mg, 34 μmol) was mixed with one mole equivalent of phosphate diester and 0.5 mL of 1.0 M perchloric acid. The mixture was warmed gently to give a clear red-purple solution and allowed to cool slowly. If crystals could not be isolated after 12 h at 4 °C, the product complex was precipitated by adding solid sodium perchlorate and recrystallized from 0.01 M perchloric acid. In some case, the complexes were oils initially. These were separated from the aqueous solution and triturated with ether, and the resulting powder was washed with ethanol and then ether, and dried with a stream of nitrogen gas (yields ranged from about 40% to 50%).

Complex 1a: δ_H (200 MHz; (CD$_3$)$_2$SO) 2.52−2.72 (12 H, m, CH$_2$), 2.80−3.18 (12 H, m, CH$_2$), 3.73 (3 H, d, *J* 11.5, CH$_3$), 6.26−6.42 (2 H, br s, NH), 6.82−7.04 (4 H, br s, NH), 7.26 and 7.30 (1 H, ArH), 7.43 and 7.47 (1 H, ArH), 8.27 (1 H, dd, J_P J_F 9.0, H2); δ_C (50.3 MHz; (CD$_3$)$_2$SO) 154.21−154.45 (m, C1), 154.17 (d, J_F 260.2, C3), 126.97 (C5), 116.01 (m, C6), 109.55 (dd, J_F 23.5, J_P 5.7, C2), 54.69 (d, *J* 5.9, POCH$_3$), 49.16−49.96 (all CH$_2$); δ_P (121.5 MHz; D$_2$O) 8.83.

Complex 1b: δ_H (200 MHz; H$_2$O) 2.7 (12H, m), 3.25 (12H, m), 3.76 (3H, d, *J* 11.4), 7.41 (2H, d, *J* 9.1), 8.31 (2H, d, *J* 9.1); δ_P (121.5 MHz; D$_2$O) 7.0 (free diester −6.8). Anal. Calcd for $C_{19}H_{39}N_7O_{20}PCo_2Cl_3$: C, 24.26; H, 4.18; N, 10.42. Found: C, 23.99; H, 4.32; N, 10.18.

Complex 1c: δ_H (200 MHz; (CD$_3$)$_2$SO) 2.56−2.62 (12 H, m, CH$_2$), 2.82−3.18 (12 H, m, CH$_2$), 3.72 (3 H, d, *J* 11.6, CH$_3$), 6.33 (2 H, bs, NH), 6.92 (2 H, br s, NH), 7.02 (2 H, br s, NH), 7.62−7.80 (2 H, m, ArH), 8.08−8.24 (2 H, m, ArH); δ_C (50.3 MHz; (CD$_3$)$_2$SO) 149.66 (d, *J* 6.7, C1), 147.08 (C3), 130.12 (C4), 125.97 (d, *J* 5.3, C2), 118.79 (C5), 114.39 (d, *J* 4.5, C6), 54.49 (d, *J* 6.0, POCH$_3$), 49.08−49.86 (all CH$_2$); δ_P (121.5 MHz; D$_2$O) 8.61.

Complex 1d: δ_H (200 MHz; CD$_3$CN) −0.95 (1 H, s, μOH), −0.93 (1 H, s, μOH) 2.45−2.70 (12 H, m, CH$_2$), 3.00−3.35 (12 H, m, CH$_2$), 3.78 (3 H, d, *J* 11.4, CH$_3$), 5.23 (2 H, br s, NH), 5.63 (2 H, br s, NH), 5.78 (2 H, br s, NH), 7.20−7.27 (3 H, m, ArH), 7.42 (2 H, t, *J* 7.8, ArH); δ_C (50.3 MHz; (CD$_3$)$_2$SO) 150.5 (d, *J* 7.2, COP), 129.8 (mC), 125.0 (pC), 120.5 (d, *J* 4.4, oC), 55.2 (d, *J* 6.0, POCH$_3$), 51.1, 50.6, 50.3, and 50.2 (all CH$_2$); δ_P (121.5 MHz; D$_2$O) 8.4 (free diester −5.5). Anal. Calcd for $C_{19}H_{40}Cl_3Co_2N_6O_{18}P\cdot H_2O$: C, 24.97; H, 4.63; N, 9.20; Co, 12.90. Found: C, 24.78; H, 4.78; N, 9.04; Co, 12.92.

Complex 2a: δ_H (200 MHz; (CD$_3$)$_2$SO) −0.72 (1 H, s, μOH), −0.67 (1 H, s, μOH), 1.05 (3 H, d, *J* 6.4, CH$_3$), 2.45−2.75 (12 H, m, CH$_2$), 2.80−3.20 (12 H, m, CH$_2$), 3.80−4.00 (3 H, m, CHCH$_2$OP), 5.35 (1 H, s, OH), 6.40 (2 H, br s, NH), 6.85 (2 H, br s, NH), 7.00 (2 H, br s, NH), 7.50 (2 H, d, *J* 7.8, ArH), 8.35 (2 H, d, *J* 7.8, ArH); δ_P (121.5 MHz; D$_2$O) 7.0 (free diester −6.9). Anal. Calcd for $C_{21}H_{43}Cl_3Co_2N_7O_{21}P\cdot H_2O$: C, 25.15; H, 4.52; N, 9.78. Found: C, 24.79; H, 4.68; N, 9.80.

Complex 2b: δ_H (200 MHz; CD$_3$CN) −0.72 (1 H, s, μOH), −0.67 (1 H, s, μOH), 1.16 (3 H, d, *J* 6.4, CH$_3$), 2.45−2.75 (12 H, m, CH$_2$), 3.00−3.35 (12 H, m, CH$_2$), 3.80−4.18 (3 H, m, CHCH$_2$OP), 4.5 (1 H, d, *J* 2.6, OH), 5.47 (2 H, br s, NH), 5.84 (2 H, br s, NH), 6.03 (1 H, br s, NH), 6.44 (1 H, br s, NH), 7.20−7.27 (3 H, m, ArH), 7.42 (2 H, t, *J* 7.8, ArH); δ_C (50.3 MHz; CD$_3$CN) 151.2 (d, *J* 7.1, COP), 130.8 (mC), 126.1 (pC), 121.2 (d, *J* 4.5, oC), 73.5 (d, *J* 6.8, POCH$_2$), 68.1 (d, *J* 5.4, HCOH), 52.1, 52.0, 51.9, 51.8, 51.7, 51.5, 51.35, 51.3 (all CH$_2$), 20.2 (CH$_3$); δ_P (121.5 MHz; D$_2$O) 7.0 (−6.9 when free). Anal. Calcd for $C_{21}H_{44}Cl_3Co_2N_6O_{19}P\cdot H_2O$: C, 26.33; H, 4.84; N, 8.77; Co, 12.31. Found: C, 26.33; H, 5.00; N, 8.61; Co, 12.13.

Complex **3** could not be isolated in a pure form as the free diester hydrolyzed at a comparable rate to the complexation reaction, and the product monoesters bind preferentially to the Co(III) centers; furthermore, none of the complexes formed could be precipitated from saturated NaClO$_4$ solution. Complex **3** could be identified at 30.44 ppm in the ^{31}P NMR, identical to material produced from **2b**. Similarly, if the cyclic ester is first hydrolyzed and then product monoesters complexed, only **5** and **5′** are produced.

Complex 4: δ_H (200 MHz; D$_2$O) 2.7 (12H, m) 3.25 (12H, m) 3.72 (6H, d, *J* 10.9); δ_P (121.5 MHz; D$_2$O) 14.3 (free diester −0.3). The crystal structure of **4** was previously reported.[3]

Kinetics. Reactions were followed at 25 °C in aqueous solution with 0.05 M buffer and $I = 0.1$ M (NaClO$_4$). Buffers used were MES (2-[*N*-morpholino]ethanesulfonic acid), HEPES (*N*-[2-hydroxyethyl]-piperazine-*N*′-[2-ethanesulfonic acid]), EPPS (*N*-[2-hydroxyethyl]piperazine-*N*′-[2-propanesulfonic acid]), CHES (2-[*N*-cyclohexylamino]-ethanesulfonic acid), CAPS (3-[*N*-cyclohexylamino]-1-propanesulfonic acid), and NaOH. As doubling the buffer concentration did not increase the observed rate constants within experimental error, extrapolation to zero buffer was not necessary.

The pK_a of the leaving group phenols was determined by titration under our experimental conditions ($I = 0.1$ M (NaClO$_4$), titrant 0.1 M NaOH), and gave values of 6.10 for *m*-fluoro, *p*-nitro phenol, 6.95 for *p*-nitro phenol, 7.95 for *m*-nitro phenol, and 9.90 for phenol. These values are used in this paper where our data are reported.

The second-order rate constants for hydroxide-catalyzed hydrolysis of the uncoordinated phosphate diesters in **1** were obtained by the initial

(6) (a) Ba−Saif, S. A.; Davis, A. M.; Williams, A. *J. Org. Chem.* **1989**, *54*, 5483. (b) Dalby, K. N.; Kirby, A. J.; Hollfelder, F. *J. Chem. Soc., Perkin Trans. 2* **1993**, 1269. (c) Brown, D. M.; Usher, D. A. *J. Chem. Soc.* **1965**, 6558.

(7) (a) Werner, A. *Justus Liebigs Ann. Chem.* **1910**, *375*, 114. (b) Wieghardt, K.; Schmidt, W.; Nuber, B.; Weiss, J. *Chem. Ber.* **1979**, *112*, 2220. (c) Siebert, H.; Tremmel, G. *Z. Anorg. Allg. Chem.* **1972**, *390*, 292.

rate method. In a typical experiment, the reaction was initiated by injection of 20 μL of a stock solution of the diester in DMSO (0.05 or 0.5 M) into 2 mL of a 0.1 M NaOH solution at a specific temperature (40, 50, 62, or 71 °C). Formation of substituted phenolate anion was monitored by following the UV−vis absorption change (phenolate, 288 nm; *m*-nitrophenolate, 390 nm; *p*-nitrophenolate, 400 nm; *m*-fluoro, *p*-nitrophenolate, 388 nm).[8] All rate constants were obtained in triplicate and were reproducible to within a few percent error. The pseudo-first-order rate constants at 25 °C were extrapolated from the Arrhenius plots.

Reactions of **1**, **2a**, and **4** were monitored by UV−vis methods. In a typical experiment, 10 μL of a 10−100 mM stock solution of complex in DMSO was added to 2 mL of buffer solution which had equilibrated in the thermostated compartment of the spectrophotometer, and the reaction was analyzed over 3 half-lives by fitting the absorbance change to a first-order exponential curve fit. Accurate first-order kinetics were observed over at least 3 half-lives in all cases. The measured pH of the final solution did not differ from the initial pH. At high pH, reaction of **4** was monitored using a stopped flow spectrophotometer, for which we are grateful to R. S. Brown, Queen's University, Kingston.

The Arrhenius parameters for **1b** were obtained by measuring the observed rate constants at 20, 25, 30, and 40 °C at pHs ~6.9, ~7.4, and ~7.8 in each case (determined by measuring the pH of the reaction mixture under the experimental conditions; the same buffer mixtures were used for each temperature). The value of k_h was calculated from each of these profiles using the appropriate value of K_w, plotted as $\ln(k_h)$ against $1/T$ and fitted to $\ln(k_h) = \ln A + E_a/(RT)$. Linear least squares regression gave the Arrhenius parameters $E_a = 49 \pm 2$ kJ mol^{-1} and $\ln A = 30.5 \pm 0.8$. These were converted to the activation parameters by applying the equations $\Delta H^{\ddagger} = E_a - RT$ and $\Delta S^{\ddagger} = R \ln A - R \ln(kTe/h) = R \ln A - 253.24$ J mol^{-1} K^{-1} (at 25 °C; k is the Boltzmann constant, and h is the Planck constant).

The deuterium solvent isotope effect for **1b** was determined at 25 °C in HEPES and EPPS buffers made up as above but with >98% deuterated water as solvent. The reaction was measured at pD 7.61, 8.09, and 8.18, where pD = pH meter reading + 0.40,[9] and gave a pD−rate profile of slope 1.

Reaction of **2b** was followed by HPLC, either by multiple injection of a buffered solution (0.2 mM), or (pH > 8) by quenching aliquots (100 μL) with pH 5.5 phosphate buffer (0.2 M, 200 μL) or MES solution (0.5 M, 200 μL) and subsequent analysis. For the quenched aliquots, rate constants were calculated from the appearance of phenol only, as diester continues to dissociate (only) under the final conditions. The multiple injection runs could be analyzed for appearance of both diester (10.2 min) and phenol (8.4 min) and disappearance of starting material (~12 min), using the same elution parameters as described below for the product analyses.

Reaction of **3** was monitored by UV−vis by allowing reaction of **2b** to proceed for 10 half-lives, and then monitoring the change in absorbance at 290 nm due to the hydrolysis/dissociation of **3** generated.

Product Analysis. For complexes **1a** and **1b**, only hydrolysis was detected by ^{31}P NMR and HPLC. For **1c**, **1d**, and **2b**, the ratio of the dissociation of the phosphate diester to the release of the substituted phenol (Schemes 1 and 4) was determined by HPLC analysis of the product solution after each kinetic run: 25 μL of the product mixture was injected onto the HPLC column and eluted with pH 5.5 ammonium phosphate buffer (0.2 M) from 0 to 5 min followed by a linear gradient to 50% methanol−water (60:40) from 5 to 12.5 min. Phenols and diesters were detected by a diode array UV−vis detector, and chromatograms were analyzed at convenient wavelengths for each species. The integrated peaks were normalized using authentic reference compounds at known concentration, allowing the observed rate constants for each run to be converted to rate constants for dissociation and hydrolysis.

Scheme 1

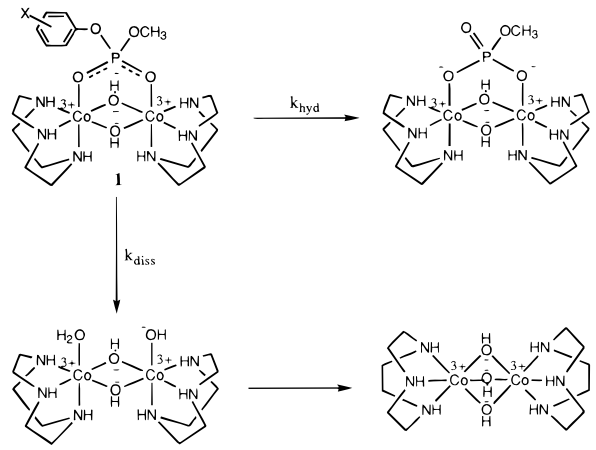

The ratio of hydrolysis to dissociation of **3** was determined by ^{31}P NMR. Initial reaction of **2b** at pH 8.2 (50 mm EPPS buffer, $I = 0.1$ M ($NaClO_4$)) reveals **3** and free diester. **3** subsequently hydrolyzes to give the two possible bound monoesters (14.15, **5**, 34%, and 13.69, **5′**, 41%) and dissociates to give the free cyclic diester (14.96, 25%) (Figure 5). Hence, the ratio of hydrolysis to dissociation is 75:25. Reaction of the free diester to produce the free cyclic diester is too slow at this pH to be observed ($k_{obs} \approx 10^{-9}$ s^{-1}).

The ratio of transesterification to hydrolysis of **2a** (Scheme 4) was determined by ^{31}P NMR, Figure 6c. A 5 mg sample of **2a** was hydrolyzed in aqueous buffer (50 mM HEPES, $I = 0.1$ M ($NaClO_4$)) at pH 8.1. After complete hydrolysis, complex **3** produced was also hydrolyzed to the two possible monoesters and free diester as above. Superimposed on this was the major product from attack of the bridging oxide, giving 14.96, free cyclic diester, 5.2%; 14.15, **5**, 85.9%; and 13.69, **5′**, 8.9%. Using the data from **3** to correct the percentage of direct attack by oxide, the ratio of transesterification to hydrolysis is calculated as 22:78.

^{18}O Labeling Experiment. Hydrolysis of **3** (generated from **2b** as described above) in 50% ^{18}O-labeled water (pH 8.2, 50 mm EPPS buffer, $I = 0.1$ M ($NaClO_4$)) was analyzed by ^{31}P NMR, Figure 6b. Complex **3** was also generated in situ from **2b** which had been synthesized with the bridging hydroxides 50% labeled with ^{18}O. The hydrolysis products (in ^{16}O water) from this reaction were also analyzed by ^{31}P NMR under the same conditions, Figure 6a.

Results and Discussion

Reactivity of 1. The bridging phosphate diesters (**1a**−**1d**) can hydrolyze (k_{hyd}), losing the substituted phenol and leaving methyl phosphate bound in the complex, or dissociate (k_{diss}) from the dinuclear Co(III) complex, which subsequently rapidly forms a triply hydroxide bridged complex, effectively making this process irreversible (Scheme 1). The overall observed rate constant (k_{obs}) for the reactions of **1a**−**1d** as determined by UV−vis methods is given by the sum of k_{hyd} and k_{diss} (eq 1). The individual rate constants were obtained from k_{obs} and the ratios of the products (phosphate diester and substituted phenol) as determined by HPLC of each kinetic run.

$$k_{obs} = k_{hyd} + k_{diss} \quad (1)$$

The rate of hydrolysis is much greater than the rate of dissociation for compounds **1a** and **1b** ($k_{hyd} \gg k_{diss}$). Hence,

(8) The rate constant for formation of *m*-fluoro-*p*-nitrophenolate is not included in Figure 3 since C−F bond cleavage is expected to occur, and so the observed value is only a maximum rate. Nucleophilic aromatic substitution of chloride and phosphate is comparable for *p*-nitro-substituted aromatic rings (Kirby, A. J.; Jencks, W. P. *J. Am. Chem. Soc.* **1965**, *87*, 3217); for hydroxide attack at phosphorus diesters with *p*-nitrophenyl or poorer leaving groups, attack at phosphorus is much faster (Kirby, A. J.; Younas, M. *J. Chem. Soc. B* **1970**, 1165, 1187). However, in protic solvents, F is substituted much more rapidly than Cl in *o*- and *p*-nitro-substituted aromatic rings (Briner, P. G.; Miller, J.; Liveris, M.; Lutz, P. G. *J. Chem. Soc.* **1954**, 1265. Bolto, B. A.; Miller, J.; Williams, V. A. *J. Chem. Soc.* **1955**, 2926) and is expected to dominate for methyl *m*-fluoro-*p*-nitrophenyl phosphate. We did not investigate this reaction further.

(9) Glasoe, P. K.; Long, F. A. *J. Phys. Chem.* **1960**, *64*, 188.

Table 1. Rate Constants for Reactions of **1**−**4**[a]

	k_h (M^{-1} s^{-1})	k_d (M^{-1} s^{-1})	$k_{d'}$ (s^{-1})	k_t (M^{-1} s^{-1})	k_f (M^{-1} s^{-1})
1a	$6.66(9) \times 10^5$				($<2.31 \times 10^{-5}$)
1b	$4.60(9) \times 10^4$				1.51×10^{-6}
1c	$2.08(3) \times 10^3$	$3.76(5) \times 10^2$	$3.06(8) \times 10^{-5}$		4.27×10^{-7}
1d	3.8(2)	$1.33(7) \times 10^2$	$3.0(3) \times 10^{-5}$		2.07×10^{-8}
2a	$7.6(1) \times 10^4$			$2.09(4) \times 10^4$	1.7×10^{-1} [6c]
2b		$1.3(1) \times 10^2$	$3.4(4) \times 10^{-5}$	$4.3(2) \times 10^2$	9.8×10^{-4} [6c]
3	$6.0(4) \times 10^1$ [b]	$2.0(2) \times 10^1$			4.7×10^{-4} [22]
4		$4.0(4) \times 10^1$			6.8×10^{-12} [13]

[a] All rate constants measured in aqueous solution, and measured at or extrapolated to 25 °C. [b] This is the observed rate constant for hydrolysis, and is the sum of the rate constants to give **5** and **5′** (see text).

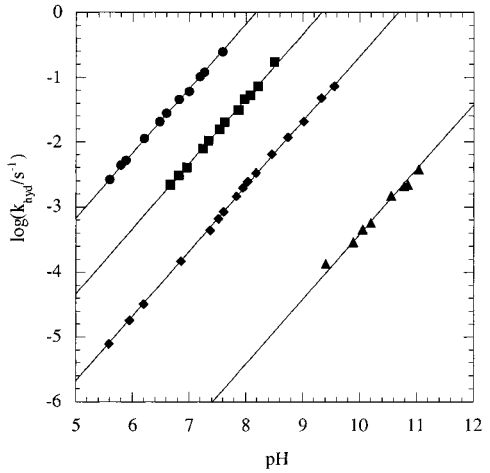

Figure 1. pH−rate profiles for the hydrolysis of **1a** (●), **1b** (■), **1c** (◆) and **1d** (▲). Linear least squares regression was used to fit these data to a slope of −1 (solid lines).

only the hydrolysis rates were measured for compounds **1a** and **1b**, with no products due to dissociation being detected. The rates of hydrolysis and dissociation are comparable for compound **1c** ($k_{diss} \approx k_{hyd}$), while for compound **1d**, the dissociation rate is greater than the hydrolysis rate ($k_{diss} > k_{hyd}$).

Figure 1 shows the pH−rate profiles for hydrolysis of the phosphate diesters in **1a** to **1d**. All four hydrolysis rates are first order in hydroxide and were fit according to eq 2. The

$$k_{hyd} = k_h[OH] \qquad (2)$$

values of k_h for compounds **1a** to **1d** are $(6.66 \pm 0.09) \times 10^5$, $(4.60 \pm 0.09) \times 10^4$, $(2.08 \pm 0.03) \times 10^3$, and 3.8 ± 0.2 M^{-1} s^{-1}, respectively (Table 1). On the basis of ^{18}O labeling experiments and a pH−rate profile for the hydrolysis reaction, we proposed that the mechanism for the hydrolysis reaction involves rate-determining nucleophilic attack of the bridging phosphate diester by the bridging oxide followed by rapid rearrangement of the intermediate to give the product (Scheme 2).[3] It follows that k_h in eq 2 is given by $K_a k/K_w$ (Scheme 2). If we assume that the value of K_a is about 10^{-15} (see below),[10] the values of k for **1a** to **1d** are $(6.66 \pm 0.09) \times 10^6$, $(4.60 \pm 0.09) \times 10^5$, $(2.08 \pm 0.03) \times 10^4$, and $3.8 \pm 0.2 \times 10^1$ s^{-1}, respectively.

We did not find any buffer catalysis for the hydroxide-catalyzed hydrolysis of **1b**. This is consistent with our proposed mechanism (Scheme 2) which involves rapid equilibrium proton

Scheme 2

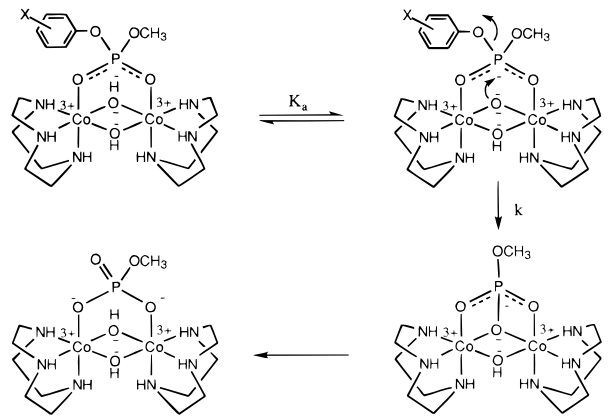

transfer (K_a) followed by rate-determining nucleophilic attack (k). The lack of buffer catalysis also indicates that there is no significant proton transfer from the solvent to the leaving group in the rate-determining step (k) as would be expected for good leaving groups. There is a small inverse solvent isotope effect (0.55) for hydroxide-catalyzed hydrolysis of **1b** (k_h in eq 2 or $K_a k/K_w$ in Scheme 2), also fully consistent with the specific base-catalyzed mechanism shown. Typical solvent isotope effects on K_a of acids are in the range of 2.5−4 (or $\Delta pK_a = 0.4-0.6$), and the isotope effect on the nucleophilic attack, k, is expected to be ∼1 (Kirby et al.[11] measured a solvent isotope effect of 1.10 for the intramolecular attack of ionized carboxylate on a phosphate diester with a good leaving group). $K_w^{D_2O}/K_w^{H_2O}$ has a value of 0.135 at 25 °C,[12] so an overall effect of 0.55 is accounted for satisfactorily if we assume that the solvent isotope effect on K_a in Scheme 2 is 3.7 ($0.135 \times 3.7 \times 1.10 = 0.55$).

We have determined the Arrhenius parameters for hydroxide-catalyzed hydrolysis of **1b** ($\Delta H^{\ddagger} = 47 \pm 2$ kJ mol^{-1}, $\Delta S^{\ddagger} = 0.4 \pm 7$ J mol^{-1} K^{-1}) and for hydroxide-catalyzed hydrolysis of the metal free diester ($\Delta H^{\ddagger} = 70 \pm 2$ kJ mol^{-1}, $\Delta S^{\ddagger} = -117 \pm 7$ J mol^{-1} K^{-1}). The more favorable entropy change in the hydrolysis of the coordinated diester is presumably due to the intramolecular nucleophilic attack of the bridging oxide on the bridging phosphate compared to the intermolecular attack of free hydroxide on the free phosphate. The more favorable enthalpy change is likely due to double Lewis acid activation of the phosphate in **1b**.

The rates of dissociation of the diesters in **1c** and **1d** were investigated in some detail. Figure 2 shows that the dissociation reaction is water catalyzed at low pH and hydroxide catalyzed at high pH. The pH−rate profiles (Figure 2) for the rate of dissociation of the diesters in **1c** and **1d** were fit according to

(10) For complex **1**, we estimate the pK_a of the bridging hydroxide as ≥15 by comparison with the pK_a for deprotonation of a hydroxide in a similar dinuclear Co(III) complex with three bridging hydroxides (Käler, H. C.; Geier, G.; Schwarzenbach, G. *Helv. Chim. Acta* **1974**, *57*, 802) and the lack of any curvature in the pH−rate profile for the reaction of **4** up to pH 14.

(11) Khan, S. A.; Kirby, A. J.; Wakselman, M.; Horning, D. P.; Lawlor, J. M. *J. Chem. Soc. B* **1970**, 1182.

(12) (a) Marshall, W. L.; Franck, E. U. *J. Phys. Chem. Ref. Data* **1981**, *10*, 295. (b) Mesmer, R. E.; Herting, D. L. *J. Solution Chem.* **1978**, *7*, 901.

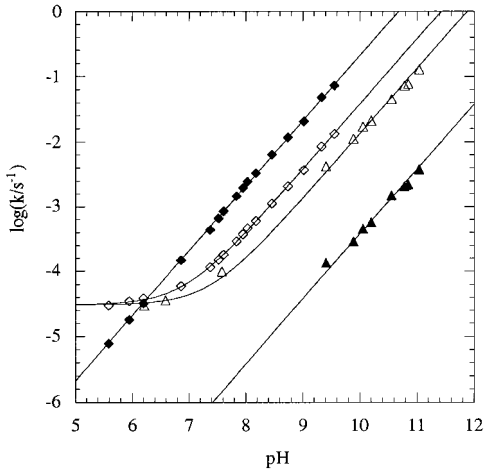

Figure 2. pH−rate profiles for the hydrolysis (filled symbols) and dissociation (open symbols) of **1c** (◆, ◇) and **1d** (▲, △). The solid lines are from the equations and rate constants described in the text.

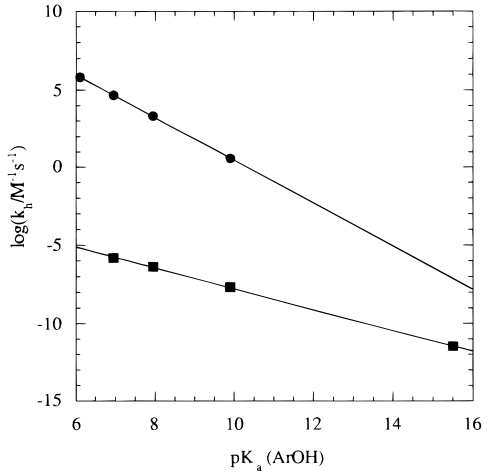

Figure 3. Linear free energy relationship between leaving group pK_a and second-order rate constant for hydroxide-catalyzed hydrolysis of compounds **1** (●; $\beta_{lg} = -1.38 \pm 0.01$; intercept 14.26 ± 0.08) and unbound diesters (■; $\beta_{lg} = -0.64 \pm 0.03$; intercept -1.4 ± 0.3). The solid lines were fitted by linear least squares regression.

eq 3. The values for k_d' and k_d are $(3.06 \pm 0.08) \times 10^{-5}$ s^{-1}

$$k_{diss} = k_d' + k_d[OH] \qquad (3)$$

and $(3.76 \pm 0.05) \times 10^2$ M^{-1} s^{-1}, respectively, for **1c** and $(3.0 \pm 0.3) \times 10^{-5}$ s^{-1} and $(1.33 \pm 0.07) \times 10^2$ M^{-1} s^{-1}, respectively, for **1d** (Table 1). It is clear from Figure 2 that compared to the dissociation reaction, the hydrolysis reaction is much more sensitive to the basicity of the leaving group.

In Figure 3, the rate constants for hydroxide-catalyzed hydrolysis of **1a** to **1d** (log(k_h)) and that of the unbound phosphates (determined by initial rate measurements under identical conditions) are plotted against the basicity of the leaving group. Interestingly, the slope (β_{lg}) of the Brønsted plot for the bound phosphates ($\beta_{lg} = -1.38 \pm 0.01$; intercept 14.26 ± 0.08; $r = 0.999\,95$) is much steeper than that for the corresponding unbound phosphates ($\beta_{lg} = -0.64 \pm 0.03$; intercept -1.4 ± 0.3; $r = 0.9988$).[8] Adding a point for dimethyl phosphate hydrolysis (3.4×10^{-12} M^{-1} s^{-1})[13] to these data gives $\beta_{lg} = -0.67 \pm 0.01$ (intercept -1.1 ± 0.1; $r = 0.9998$). Hence, a much greater rate acceleration is expected for the hydrolysis of phosphates with good leaving groups than for hydrolysis of phosphates with poor leaving groups. A potential way of exploiting this may be to make a leaving group effectively much better through coordination to another metal ion, or through efficient general acid catalysis; these combinations should give strong cooperative effects in promoting hydrolysis.

(13) After statistical correction for two identical leaving groups. See: Guthrie, J. P. *J. Am. Chem. Soc.* **1977**, *99*, 3991.

Scheme 3

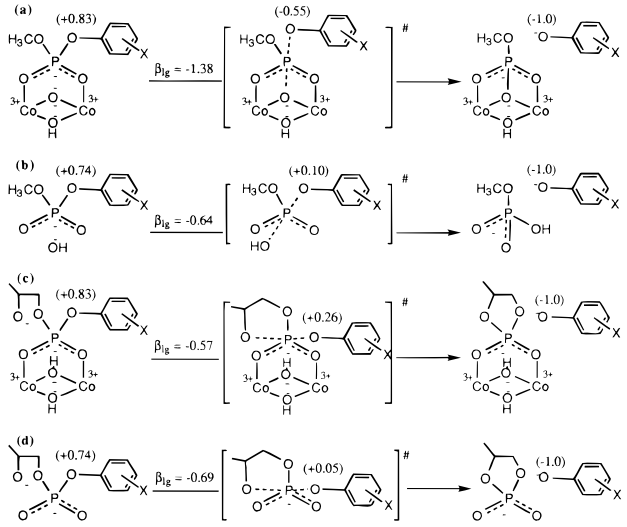

We can estimate the extent of P−O bond cleavage at the transition state for the hydrolysis of **1a** to **1d** as follows (Scheme 3a).[14] The amounts of charge on the phenolic oxygen in phenolate anion, in singly protonated phenyl phosphate, and in doubly protonated phenyl phosphate are −1, 0.74, and 0.83, respectively.[15] If we assume that the amount of charge in the phenolic oxygen of **1d** is about the same as that in doubly protonated phenyl phosphate,[16] the total change in the charge upon hydrolysis of **1d** is expected to be $-1 - 0.83 = -1.83$. Since the value of β_{lg} is −1.38 for the hydrolysis of **1a** to **1d**, the extent of P−O bond cleavage at the transition state for the reactions is estimated to be about $-1.38/-1.83 = 0.77$. The relative charge of the phenolic oxygen at the transition state is expected to be about $0.83 - 1.38 = -0.55$.

Using a similar analysis, the extent of P−O bond cleavage for the hydrolysis of the corresponding unbound phosphates is expected to be about $-0.64/-1.74 = 0.37$ (Scheme 3b). Hence, the transition states are much more advanced for the hydrolysis of the bound phosphates than those for the hydrolysis of the unbound phosphates.

The greater value of β_{lg} for the hydrolysis of **1** compared to that for hydroxide-catalyzed hydrolysis of the free diester is due to greater P−O bond cleavage at the transition state for the former reaction. This results in greater rate acceleration for the hydrolysis of the diester with better leaving groups (Figure 3). The large value of β_{lg} in Figure 3 is unusual for attack at a phosphate diester with a good leaving group by a nucleophile with a high basicity. For attack of analogous phosphate triesters by a poor nucleophile such as water, a β_{lg} of −1.0 is observed, which decreases to −0.35 for hydroxide attack.[17] Similarly, for phosphate diester hydrolysis catalyzed by nucleophilic attack

(14) (a) Williams, A. *Acc. Chem. Res.* **1984**, *17*, 425. (b) Williams, A. *Chem. Soc. Rev.* **1986**, *15*, 125.

(15) Bourne, N.; Williams, A. *J. Org. Chem.* **1984**, *49*, 1200.

(16) Binding phosphate or carboxylate to two Co(III) centers has the same effect as a single protonation. (a) Edwards, J. D.; Foong, S.-W.; Sykes, A. G. *J. Chem. Soc., Dalton Trans.* **1973**, 829. (b) Scott, K. L.; Green, M.; Sykes, A. G. *J. Chem. Soc. A* **1971**, 3651.

(17) Khan, S. A.; Kirby, A. J. *J. Chem. Soc. B* **1970**, 1172.

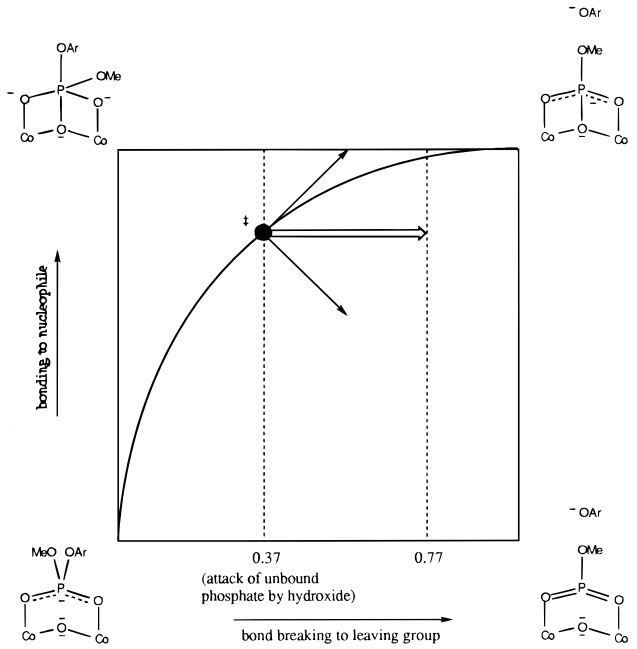

Figure 4. More O'Ferrall−Jencks diagram for the hydrolysis of compounds **1**. The circle represents the transition state for intermolecular attack by hydroxide, and the small arrows show the Hammond and anti-Hammond movements that result when the diester is complexed in **1**. The resultant transition state movement is shown by the large arrow.

Scheme 4

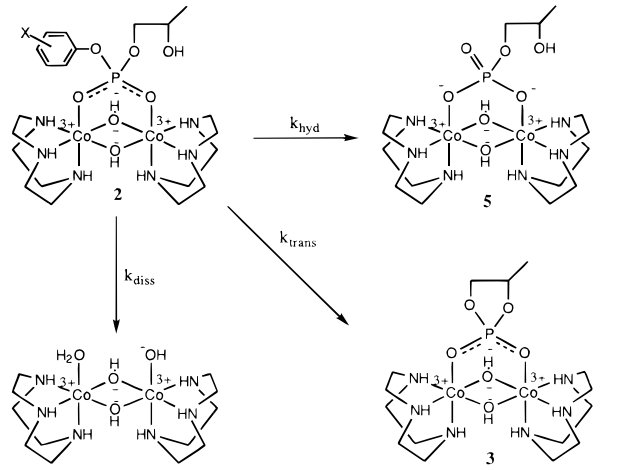

of an intramolecular carboxylate, Kirby et al.[11] measured a β_{lg} of −1.26, whereas in this work we find that hydroxide attack at methyl aryl phosphates has a β_{lg} of −0.64. We explain this observation in terms of a More O'Ferrall−Jencks energy diagram,[18] where the *y*-axis in Figure 4 represents P−O bond formation between the oxide and the phosphate and the *x*-axis represents P−O bond cleavage from the expulsion of the leaving group. Nucleophilic attack of the oxide on the phosphate results in formation of two four-membered rings. The strain in the two four-membered rings destabilizes the two top corner species in Figure 4, shifting the position of the transition state toward the top right corner (Hammond effect) and to the bottom right corner (anti-Hammond effect).[19] The vector sum of these two effects should move the transition state toward greater P−O bond cleavage and hence a great value of β_{lg}. Similarly, the cleavage of phosphate diesters and triesters with weaker nucleophiles should also result in destabilization of the top two corner species, giving the high values of β_{lg} measured by Kirby et al.[11]

(18) (a) More O'Ferrall, R. A. *J. Chem. Soc. B* **1970**, 274. (b) Jencks, W. P. *Chem. Rev.* **1972**, *72*, 705.

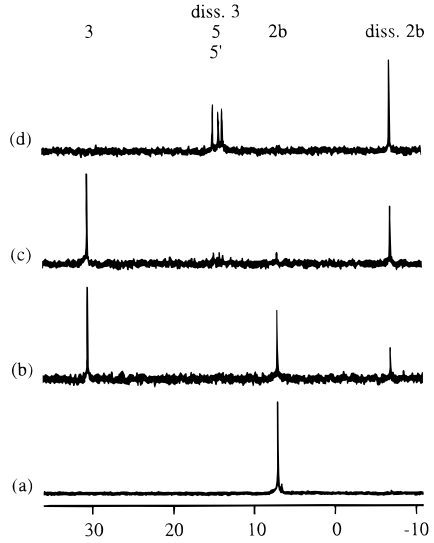

Figure 5. ^{31}P NMR spectra for the hydrolysis of **2b**. (a) In 0.01 M $HClO_4$ in D_2O and then at pH 8.2 after (b) 18 min, (c) 52 min, and (d) 3 h (heating to 50 °C for final 30 min). "diss. 2b" and "diss. 3" refer to the free diesters released by dissociation of complexes **2b** and **3**, respectively.

Reactivity of 2. The cause of the above shift in the transition state was further investigated by studying intramolecular transesterification of diesters coordinated to the same dinuclear center. This allows the effect of double Lewis acid activation on the transition state to be measured separately. The phosphate diesters in **2a** and **2b** can hydrolyze (k_{hyd}) or dissociate (k_{diss}) like the phosphate diesters in **1a** to **1d**. Additionally **2a** and **2b** can undergo intramolecular transesterification (k_{trans}) to form the bridging cyclic phosphate diester **3** (Scheme 4). The overall rate constant (k_{obs}) for the reactions of **2a** and **2b** is given by eq 4, and the individual rate constants again determined from k_{obs} through product analysis, in this case a combination of HPLC and ^{31}P NMR (Figures 5 and 6).

$$k_{obs} = k_{hyd} + k_{diss} + k_{trans} \quad (4)$$

For compound **2a**, the rates of the transesterification and hydrolysis reactions are much faster than the rate of the dissociation reaction (k_{trans}, $k_{hyd} \gg k_{diss}$), with no dissociation product observed. Hydrolysis of **2a** results in formation of the bridging phosphate monoester (**5**, Scheme 4) while transesterification of **2a** results in formation of the bridging cyclic phosphate diester (**3**). The rates of hydrolysis and transesterification of **2a** are given by eqs 2 and 5, respectively. Best fits gave $k_h = (7.6 \pm 0.1) \times 10^4$ M^{-1} s^{-1} and $k_t = (2.09 \pm 0.04) \times 10^4$ M^{-1} s^{-1} for **2a** (Table 1).[20]

$$k_{trans} = k_t[OH] \quad (5)$$

(19) We assume a concerted mechanism based on the results of Hengge and Cleland (Hengge, A. C.; Cleland, W. W. *J. Am. Chem. Soc.* **1990**, *112*, 7421). These authors showed that hydroxide-catalyzed hydrolysis of phosphates with good leaving groups takes place by a concerted mechanism. According to the principle of microscopic reversibility, a weak nucleophile should also cleave phosphates by a concerted mechanism.

(20) It is unlikely that the bridging oxide acts as a general base for the transesterification reaction since the basicity of the oxide is expected to be greater than the basicity of the alkoxide formed from **2**.

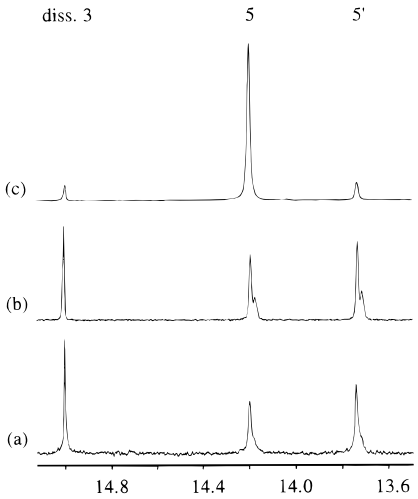

Figure 6. ^{31}P NMR spectra for the hydrolysis of **2a** and **3**. (a) **3** after hydrolysis at pH 8.2 with bridging OH 50% labeled with ^{18}O. (b) **3** after hydrolysis at pH 8.2 in 50% ^{18}O-labeled H_2O. (c) **2a** after hydrolysis at pH 8.2. "diss. 3" refers to the free diester released by dissociation of complex **3**.

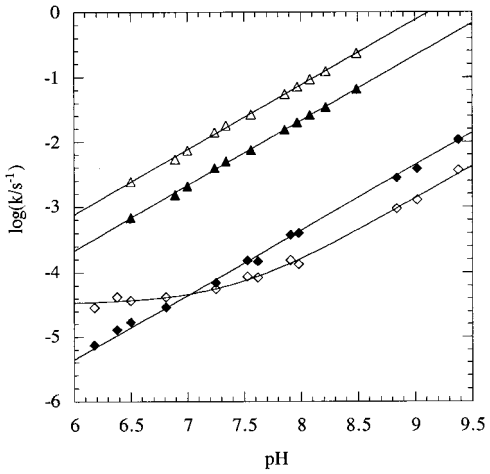

Figure 7. pH rate profiles for the transesterification, hydrolysis, and dissociation of **2a** (△, hydrolysis; ▲, transesterification) and **2b** (◇, dissociation; ◆, transesterification). The solid lines are from the equations and rate constants described in the text.

For compound **2b**, the rates of the transesterification and dissociation reactions are much faster than the rate of the hydrolysis reaction (k_{trans}, $k_{diss} \gg k_{hyd}$), with none of the hydrolysis product being detected (Figure 5). Hence, only the rates of transesterification and dissociation were determined for **2b**; this is consistent with the rates obtained for the hydrolysis and dissociation of **1d**, which has the same leaving group. The rate of hydrolysis of **2b** by nucleophilic attack of the phosphate diester by the bridging oxide should be comparable to that for **1d**. The rates of dissociation and transesterification of **2b** are given by eqs 3 and 5, respectively. Best fits gave $k_d = (1.3 \pm 0.1) \times 10^2$ M^{-1} s^{-1}, $k_d' = (3.4 \pm 0.4) \times 10^{-5}$ s^{-1}, and $k_t = (4.3 \pm 0.2) \times 10^2$ M^{-1} s^{-1} for **2b** (Table 1). The data for transesterification, hydrolysis, and dissociation of **2a** and **2b** as a function of pH are shown in Figure 7.

In Figure 8, the rates of transesterification of **2a** and **2b** and that of the uncoordinated 2-hydroxypropyl aryl phosphates[6c] are plotted against the basicity of the leaving group. The rates of hydrolysis of uncoordinated methyl aryl phosphates are also plotted in the same figure for comparison. The 2-hydroxypropyl group provides about 5 orders of magnitude rate acceleration for the cleavage of the phosphate diester regardless of the

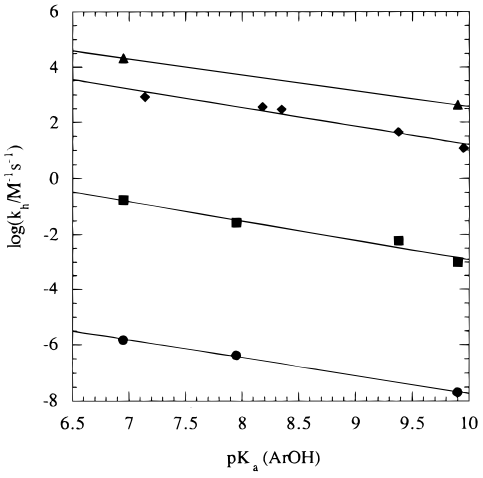

Figure 8. Linear free energy relationships between leaving group pK_a and second-order rate constants for hydrolysis or transesterification catalyzed by hydroxide for methyl aryl diesters (●), 2-hydroxypropyl aryl esters (■), **6** (◆) and **2** (▲).

leaving group. Double Lewis acid activation provides about another 5 orders of magnitude rate acceleration for the cleavage reaction, again largely independent of the basicity of the phosphate diester leaving group. Thus, these two effects are close to additive for good and poor leaving groups. In contrast, the bridging oxide contributes a much greater rate acceleration for cleaving **2a** than for cleaving **2b** as expected from the large value of β_{lg} for the hydrolysis of **1a**−**1d** (Figure 3). The reactivity of the bridging oxide in **2b** is much less than that of the hydroxypropyl group and could not be measured. However, the bridging oxide in **2a** is more reactive than the hydroxypropyl group and can easily be measured (Table 1).

We have also included the data for hydroxide-catalyzed transesterification of **6** (omitting data for ortho-substituted phenols) in Figure 8.[21] The slope of this Brønsted plot is approximately parallel to that of the other three over the same range in the pK_a of the leaving group. Our dinuclear Co(III) complex should provide 5−6 orders of magnitude rate acceleration for the transesterification of **6**, regardless of the leaving

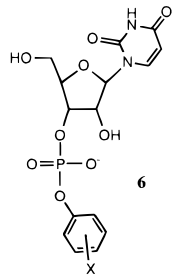

6

group. The second-order rate constant for hydroxide-catalyzed transesterification of UpU, extrapolated to 25 °C, is 3.2×10^{-3} M^{-1} s^{-1}.[22] Hence, the second-order rate constant for hydroxide-catalyzed transesterification of a typical RNA phosphate diester bridged to the dinuclear Co(III) complex should be about 10^3 M^{-1} s^{-1}. At neutral pH, the half-life of the phosphate diester bond of RNA should be reduced from about 100 years to within a few hours upon coordination to the dinuclear Co(III) complex.

(21) Davis, A. M.; Hall, A. D.; Williams, A. *J. Am. Chem. Soc.* **1988**, *110*, 5105.

(22) Järvinen, P. ; Oivanen, M.; Lönnberg, H. *J. Org. Chem.* **1991**, *56*, 5396. Rate constant extrapolated from the data given for UpU hydrolysis at 90 and 60 °C. Also see, Kuusela, S.; Lönnberg, H. *J. Chem. Soc., Perkin Trans. 2* **1994**, 2109.

Scheme 5

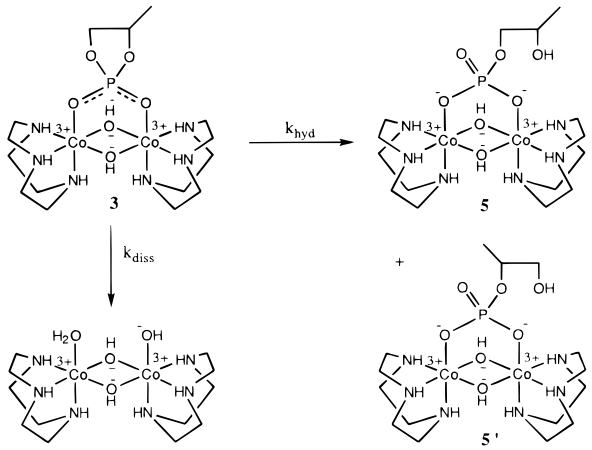

Scheme 6

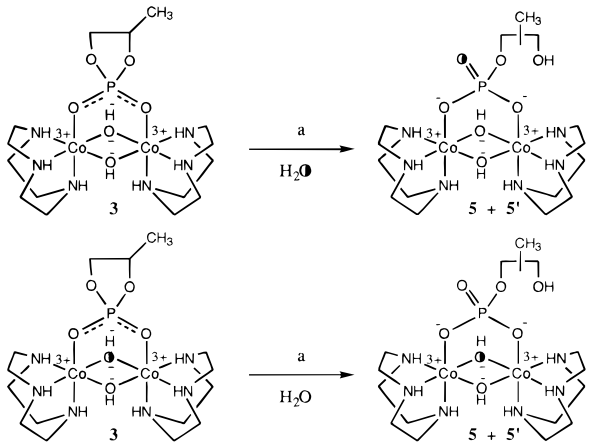

The extent of P−O bond cleavage at the transition state for the transesterification of **2a** and **2b** can be estimated as 0.28 (Scheme 3c), again assuming that complexation to the dinuclear Co(III) center has an effect similar to that of protonation of the unbound diester ($\beta_{lg} = -0.57$; final charge on leaving group oxygen −1; initial charge on leaving group oxygen +0.83; extent of cleavage at transition state $-0.57/(-1 - 0.83) = 0.28$). Hence, double Lewis acid activation alone does not shift the transition state to greater P−O bond cleavage, as the comparable calculation for the unbound diester gives $-0.69/(-1 - 0.74) = 0.40$ (Scheme 3d). Thus, if anything, double Lewis acid activation yields a slightly more associative transition state for transesterification. Double Lewis acid activation alone is expected to stabilize the top two corner species and shift the transition state to lesser P−O bond cleavage (Figure 4). It is the bridging oxide that shifts the transition state to greater P−O bond cleavage.

Reactivity of 3. The expectation (based on Figure 8) that double Lewis acid activation should provide similar rate accelerations with widely varying diesters is borne out by studying the reactions of the intermediate **3**. The bridging cyclic phosphate diester (**3**) can hydrolyze (k_{hyd}) or dissociate (k_{diss}) much like compounds **1a** to **1d** (Figure 5). The hydrolysis reaction results in formation of the bridging phosphate monoesters **5** and **5′** in a ratio of about 45:55 (Scheme 5). The second-order rate constants for the hydroxide-catalyzed hydrolysis and dissociation reactions for **3** are 27 ± 3 M^{-1} s^{-1} to give **5**, 33 ± 3 M^{-1} s^{-1} to give **5′**, and 20 ± 2 M^{-1} s^{-1}, respectively.

The second-order rate constant for hydroxide-catalyzed hydrolysis of the cyclic ethylene phosphate is 2.35×10^{-4} M^{-1} s^{-1}.[23] Hence, the coordinated phosphate diester in **3** is hydrolyzed about 1.3×10^5 times more rapidly than the corresponding uncoordinated cyclic phosphate. To determine if this acceleration was still due to a combination of intramolecular nucleophile and double Lewis acid activation, as for **1a** to **1d**, ^{18}O labeling experiments were performed in which the solvent and bridging hydroxyls were labeled with 50% ^{18}O in turn (Scheme 6).

The incorporation of ^{18}O into phosphates can be detected by ^{31}P NMR spectroscopy since it results in an upfield shift of the phosphate signal by about 0.02 ppm.[24] ^{31}P NMR analysis of the products of these reactions (Figure 6b,c) revealed that attack by the bridging oxide is not the major mechanism, in direct contrast to the result of similar experiments with **1b**.[3] Extrapolating (using the data in Figure 3) the rate accelerations between bound and unbound diesters to a leaving group pK_a of 14.8[25] gives a predicted acceleration of $\sim 4 \times 10^4$ which is slightly less than expected from double Lewis acid activation alone, as measured with compounds **2a** and **2b**. Thus, we propose that the intermolecular reaction shown in Scheme 6 now dominates. Although the NMR analysis could not be sufficiently resolved to give baseline resolution of the labeled products, nor to conclusively show that no label at all is incorporated from the bridging nucleophile, it is clear that at least the majority of the nucleophile is supplied by solvent. Comparing the predicted and measured accelerations indicates that 70% of the reaction is through attack by solvent, and 30% by bridging oxide. This in turn predicts 35% incorporation from the solvent labeling experiment, and 15% from the bridge labeling experiment, which agrees well with the observed NMR results. This analysis gives a rate acceleration for the intermolecular reaction of $\sim 1 \times 10^5$, which agrees well with that measured for the transesterification reactions described above despite the changes from good to poor leaving group, and from intra- to intermolecular nucleophile. Clearly, the efficiency of the bridging oxide has diminished so much with the poorer leaving group that the intermolecular reaction has taken over as the favored reaction.[26]

Reactivity of 4. The rate of hydroxide-catalyzed hydrolysis of dimethyl phosphate (3.4×10^{-12} M^{-1} s^{-1})[13] is over 10^{12}-fold slower than the rate of hydroxide-catalyzed dissociation of phosphate diesters from the dinuclear Co(III) complexes (k_d, Table 1). The rate of hydrolysis of dimethyl phosphate in **4** is expected to be millions of times slower than the dissociation rate since the dinuclear Co(III) complex should provide only double Lewis acid activation (10^5−10^6-fold rate enhancement) for hydrolyzing phosphates with poor leaving groups. Indeed, we do not observe any hydrolysis of the phosphate diester bond in **4**. The rate of hydroxide-catalyzed dissociation of dimethyl phosphate from **4** was measured up to 1 N NaOH by stopped flow methods. The rate increased linearly with an increase in hydroxide concentration, indicating that the pK_a of the bridging

(23) After statistical correction for two identical leaving groups. See: Kumamoto, J.; Cox, Jr., J. R.; Westheimer, F. H. *J. Am. Chem. Soc.* **1956**, *78*, 4858.

(24) (a) M. Cohn, M.; Hu, A. *Proc. Natl. Acad. Sci. U.S.A.* **1978**, *75*, 200. (b) Lowe, G.; Sproat, B. S. *J. Chem. Soc., Chem. Commun.* **1978**, 565.

(25) The pK_a of ethylene glycol is 14.8 (Jencks, W. P.; Regenstein, J. *Handbook of Biochemistry and Molecular Biology*; CRC Press: Cleveland, 1976; p 159).

(26) Comparing the lines in Figure 3, the acceleration due to the combination of double Lewis acid activation and oxide attack depends very strongly on the leaving group pK_a: log(acceleration) = $15.61 - 0.74$pK_a. Thus, for leaving group pK_a values >14.3, external hydroxide attack on the phosphate is favored over the internal oxide attack.

hydroxides in **4** is greater than 14, in accordance with an estimated pK_a of ~15.[10]

Cooperativity between Oxide Activation and Leaving Group Activation. The present study indicates that for hydrolyzing unactivated phosphate diesters with the dinuclear Co(III) complex in **1**, there should be a considerable synergistic effect between the oxide nucleophilic attack and leaving group activation (such as coordination of the leaving group oxygen to a metal ion). If a third metal were to coordinate to the leaving group oxygen and lower the pK_a of the leaving alcohol from about 14 to 4, this leaving group activation in isolation would provide only about 6.4 orders of magnitude rate acceleration (Figure 3, lower slope 0.64). The nucleophile activation in isolation provides no rate acceleration for poor leaving groups; as shown above, the dinuclear Co(III) complex provides only about 5 orders of magnitude rate acceleration (due to double Lewis acid activation) for hydrolyzing phosphates with poor leaving groups. The above leaving group activation *together* with the oxide nucleophile activation should provide 13.8 orders of magnitude (Figure 3, upper slope 1.38) rate acceleration for the hydrolysis reaction. Hence, the leaving group activation and the nucleophile activation is not simply additive in this case, with the cooperative effect between the leaving group activation and the nucleophile activation providing an additional 7.4 orders of magnitude rate acceleration ($13.8 - (6.4 + 0) = 7.4$). In the above example, the total rate acceleration due to double Lewis acid activation, leaving group activation, and nucleophile activation would be $13.8 + 5 = 18.8$ orders of magnitude! This would be enough to bring down the half-life of the phosphate diester bond of DNA from tens of billions of years to within seconds (at pH 7, 25 °C).[27]

In conclusion, phosphate diesters coordinated to a dinuclear Co(III) complex can be rapidly hydrolyzed through double Lewis acid activation and an intramolecular oxide nucleophile that bridges the two metal ions. While double Lewis acid activation provides comparable rate accelerations over the background hydroxide rate for cleaving phosphate diesters with good or poor leaving groups, the oxide nucleophile provides increasingly greater rate acceleration for cleaving phosphate diesters with better leaving groups. This behavior can be understood in terms of a More O'Ferrall−Jencks energy diagram, and it indicates that there will be enormous cooperativity between the oxide activation and leaving group activation.

Acknowledgment. We thank the NSERC, Pioneer Hi-Bred International Inc., and the U.S. Army Research Office for support of this work.

JA980660S

(27) DNA or RNA has not as yet been attached to the dinuclear Co(III) compound.